Characterization of Bi_2Te_3 Nanostructure by Using a Cost Effective Chemical Solution Route

Mamur, Hayati*[+]

Department of Electrical and Electronics Engineering, Manisa Celal Bayar University, 45140, Manisa, TURKEY

Bhuiyan, Mohammad Ruhul Amin

Department of Electrical and Electronic Engineering, Islamic University, 7003, Kushtia, BANGLADESH

ABSTRACT: *An efficient and cost effective approach in the synthesis process of the bismuth telluride (Bi_2Te_3) powders and pellets were developed based on a chemical solution route. The route consists of dissolving of both the bismuth (III) nitrate pentahydrate, $Bi(NO_3)_3.5H_2O$ and tellurium dioxide, TeO_2 into the same inorganic nitric acid, HNO_3 with the two–step precipitation of sodium hydroxide, NaOH and sodium borohydride, $NaBH_4$. The different characterization parameters such as X–Ray Diffraction (XRD), Scanning Electron Microscopy (SEM), Energy Dispersive X–ray (EDX), Transmission Electron Microscopy (TEM), Atomic Force Microscopy (AFM), UltraViolet (UV) absorbance and Fourier Transform InfraRed (FT-IR) spectrometry were carried out. As a result of these, the developed powders possessed a rhombo-hedral crystal structure exhibiting a nanocrystalline form with crystalline size about 10 nm. The elemental of Bi and Te were developed with their stoichiometric atomic ratio of (30.15):(48.19). Furthermore, the TEM micrographs showed an aggregate phenomenon and the primary crystalline size being quite low. Additionally, the produced Bi_2Te_3 pellets indicated a smooth surface with an average roughness value of 58 nm according to the AFM image. Absorption has occurred at about a range within 1 (arbitrary unit). Ultimately, the FTIR demonstrated that the C–H, O–H, C–O and C–S bonds were similar to the Bi_2Te_3 nanostructure materials.*

KEYWORDS: *Bi_2Te_3; Chemical solution route; Nanostructure materials; Nanocrystalline form.*

INTRODUCTION

Bismuth telluride (Bi_2Te_3) is a semiconductor type material that is a compound of bismuth (Bi) and tellurium (Te). When the post–transition metal element of Bi alloys with a metalloid non–metal element of Te, it behaves like an acceptable ThermoElectric (TE) semiconductor material [1]. Recently, it has taken a great deal of fascinating attention from energy harvesting to chip cooling and sensing [2]. TE power generation devices perform a crucial role for utilization in the geothermal and solar power areas.

TE generators and their parameter measurements have been presented some studies [3–5]. According to these reports, ThermoElectric Generators (TEGs) have less than

* *To whom correspondence should be addressed.*
+ *E-mail: hayati.mamur@cbu.edu.tr*
1021-9986/2020/3/23-33 11/$/6.01

10% efficiency. In order to increase the efficiency, a great deal of studies has been carried out [6]. These studies have been focused on the nanostructure materials. Therefore, many techniques have been used to produce Bi_2Te_3 nanostructure. In authors' previous reports [7, 8], a growth technique was proposed to produce the device quality materials of the Bi_2Te_3 nanostructure.

Development of the nanostructure TE materials is firmly connected to the capability to find out the micro-structural and optical characterization such as orientation, nanocrystalline size, elemental stoichiometric, surface homoniginity, absorbance and volumetric ratio. But, the nanostructure material characterization is more difficult compared to the thin films. In order to achieve the nanostructure material characterization, some developed microscopic devices are used [9]. A Transmission Electron Microscopy (TEM) is one of them. The TEM assures an explicit measurement of the nanostructure materials [10]. The same remark can be said to an Atomic Force Microscopy (AFM). Furthermore, X–Ray Diffraction (XRD) can determine the imperceptible volumes and is so much accessible for texture inquiry. However, the XRD has minimum capabilities for a crystalline size assessment. The crystalline size assessment analyser established on laser beam diffraction is intensely used in the nanostructure materials. Other spectroscopy can be recycled as an additional tool for the nanostructure material investigation because the rate of the Internal Friction (IF) is nearly associated to the material structure. But, definitive empirical data has been possessed so far on TE alloys.

Taking into account for all of these, so many investigation enterprises on Bi_2Te_3 nanostructure were grown by using the different techniques like evaporation-condensation, sputtering, pulsed laser ablation, chemical, electrochemical, solvothermal and hydrothermal [11-14]. The chemical routes are available for the synthesis of nanostructure Bi_2Te_3 [15-18]. In the literature reports, the authors have used the different organic reagents such as ethylenediamintetraacetice acid disodium salt (EDTA), ethylene glycol EG $(OH)C_2H_2(OH)$, polyvinyl pyrrolidone (K30) PVP, hydrazine hydrate $N_2H_4.H_2O$, ascorbic acid $C_6H_8O_6$. In this study, to prepare the solutions, only the inorganic HNO_3 instead of these organic materials has been used because the $Bi(NO_3)_3.5H_2O$ and TeO_2 easily dissolve in HNO_3. According to the authors' previous review reports, a route has been presented for producing the efficient Bi_2Te_3 nanostructure. By means of the study, their implementations [19, 20] have been executed. The effect of organic and alkali modifiers on the crystal structure of any materials have been shown.

The main difference between this work and literature reports is that only one material has used for preparing the solution. For this reason, it has lots of advantages such as a sensitive control of the crystalline dimension, structure distribution and crystallinity of the end product of precursors. Also, it offers a significant enhancement for the chemical activities of the reactant, the possibility to replace the solid state method, and materials. Moreover, products of an intermediate state, a metastable state and a specific phase could be easily fulfilled by means of the process. Therefore, the proposed process is a cost effective synthesis technique. In order to complete the characterization of the nanostructure of Bi_2Te_3 powders and pellets produced by a cost effective chemical solution route, some of these studies have been demonstrated in this paper. Further research will be recommended to study the TE properties of Bi_2Te_3 nanostructures.

EXPERIMENTAL SECTION

Developing of the nanostructure Bi_2Te_3

The reagents of $Bi(NO_3)_3.5H_2O$ (≥98%, Sigma–Aldrich) and TeO_2 (≥97%, Sigma–Aldrich) were purchased form Sigma–Aldrich and used as starting materials for the co–precipitation of a chemical solution route. The solvents of HNO_3 (65%, Sigma–Aldrich), NaOH (98–100%, Sigma–Aldrich), $NaBH_4$ (98–100%, mark) and Ethanol (Analytical grade, Mark) were also purchased and used without further purification. These chemicals were weighted according to their stoichiometry (Bi_2Te_3) and prepared separate metal ion solutions by using 4 mmol (1.94 gm) $Bi(NO_3)_3.5H_2O$ and 6 mmol (0.9576 gm) TeO_2. These were dissolved in the concentrated (2 M=31.86 ml) HNO_3. The NaOH, a stock solution of (3 M=30 gm) was employed for regulating pH value. In authors' previous report [7], the developed procedure of the Bi_2Te_3 nanostructure was utilized. According to the procedure, firstly, $Bi(NO_3)_3.5H_2O$ + 2 M HNO_3 and TeO_2 + 2 M HNO_3 were mixed together with solution 1. Then, the white precipitates (Solution 3)

were prepared with Solution 1 and 3M NaOH (Solution 2). After that, the black precipitates were generated with solution 3 and $NaBH_4$ (Solution 4). Finally, the nanostructure Bi_2Te_3 powders and pellets were successfully developed by using a chemical solution route.

Experimental technique

Firstly, the XRD patterns were recorded by using a X'Pert high score PANalytical diffractometer with Cu–Kα radiation operated at 45 kV and 40 mA with angular range $10^o \leq 2\theta \geq 80^o$. Next, the morphology and atomic compositions (elemental) of the sample were also consummated with a SEM and an EDX of LEO 1430 VP systems. Then, the TEM measurement was performed for understanding the morphology changes of the synthesized Bi_2Te_3 nanostructure with the field emission TEM using JEOL JEM 2100F HRTEM microscope operated at 200 kV. After that, the 3D topographic surfaces were recorded in 0.01 nm discrimination using 10 MP CCD cameras by an AFM. In addition, the UV absorption was measured by using a UV–1800 recording spectrophotometer in the photon wavelength range between 200 and 800 nm. Finally, a Bruker Tensor II spectrometry was used for FTIR measurements.

RESULTS AND DISCUSSIONS

Simply by changing the reaction conditions, resides that a remarkable aspect of a chemical solution route versatility such as metals, oxides, sulphides and carbides can be prepared in various nanostructure forms. By using the bottom up approaches, it is based on the handling of the molecules and atoms to construct the compound TE materials. The formation of the white precipitate occures from a homogeneous liquid phase because of a physical conversion and a chemical solution. In almost every case, the construction of advanced solid phase in a liquid medium simultaneously outcomes by nucleation and agglomeration of the particles [21]. In homogeneous solutions, the growth of nanosize particle can be regulated by controlling of the cations and anions. In addition, the kinetics of the precipitation and careful handling of the results can be developed for the monodisperse nanosize particles. By adjusting the circumstances, the particles with nanostructured distributions can be formed to determine the precipitation preceding such as the pH of solution and concentration of the reactants [22]. For the Bi_2Te_3 synthesis process, the co–precipitation involves with the precipitation of hydroxides by the addition of a NaOH solution indicating the solution of raw material. It is noted that the reaction chemistry applicable to the co–precipitation of Bi and Te described herein leads to the hypothesis that the white colour precursor is most likely a hydrated, very confidential mixture of Bi and Te. Thus, it demonstrated the advantage of control allowing over the stoichiometry of materials by using the homogeneous sample production and easily composite materials preparation.

Additionally, the metal solution is carried out by direct reaction between $Bi(NO_3)_3.5H_2O$ and TeO_2 in the inorganic solution of HNO_3. It is reasonably studied that TeO_2 and $Bi(NO_3)_3.5H_2O$ can be converted into Te^{2-} and Bi^{+3} by HNO_3. The expected chemical reaction is Bi^{3+} ions to associate with the reduced Te^{2-} ions to combine to form the Bi_2Te_3 during this chemical reaction as below:

$$Bi(NO_3)_3.5H_2O \text{ (heat } \sim 70^o \text{ to } 80^oC) \rightarrow 3H_2O + 2HNO_3 + BiNO_3(OH)_2$$

$$2TeO_2 + HNO_3 \rightarrow Te_2(NO_3)O_3(OH)$$

$$NaOH + HNO_3 \rightarrow NaNO_3 + H_2O$$

$$2Bi_2O_3 + 9TeO_3 + 6NaBH_4 \rightarrow 2Bi_2Te_3 + 3NaTeO_3 + 6H_2BO_3 + 6H_2O$$

This solution route has many advantages such as simple solution, faster producing, low–cost and utilization of the non-toxic materials. Furthermore, it allows the product to be free from other anions because herein it use the inorganic solutions having a low relative permittivity. Moreover, the production of TE materials at the molecular level offers a number of advantages by using the chemical solution route that can develop better homogeneity for multiphase materials and a cost effective bulk quantity production. Additionally, it allows the control of crystalline size and growth agglomeration at a molecular level. For these reasons, it might be possible to minimise the cost and efficiency for the production of the ultra–fine device quality Bi_2Te_3 nanopowders. According to previous report [23], this route has been monitored the best performance for producing the nanostructure powders when compared with thin films and electrochemical synthesis. Ultimately, both low toxicity and a cost effective solution are used by performing this route.

The advancement of these TE materials into next generation appliances crucially depends on understanding of the relationship between structure and characteristics. In this context, the XRD provides a quite well complimentary message about the nanostructure materials by showing the average coherence length as a function of direction. Its results give an overall view of the nanostructure form that is average over a large volume. The length of structural coherence between one and several tens of nanometers shows the nanostructure materials. A nanostructure material acts as a grating to a certain expansion. It produces the XRD pattern which shows a diffuse component and peaks. However, these peaks are observed in the XRD patterns of regular crystals. In addition, the diffuse components indicate a very strong with the non–crystalline structure. Fig. 1 illustrates the XRD spectra of the prepared Bi_2Te_3 powder materials.

The XRD spectra of the prepared sample demonstrated that the main reflections were quite well index to the reference code and matched to rhombohedra Bi_2Te_3 nanostructure (Reference Code 98–018–4631 which provides XRD machine for Bi_2Te_3 powder diffraction standards data same as JCPDS). There were not other crystalline impurities detected that indicating the phase purity of the Bi_2Te_3 powders. The spectrum showed that the structure indicated the nano crystalline with a (015) identified orientation (peak having sharp and higher intensity). When the spectrum with the Bi_2Te_3 nanostructure was compared the standard reference code, corresponding to (101), (015), (1010), (0111), (110) (205), (1016), (0210), (1115), (125), (2110) and (1211) planes, these were seen similar. These were in very good agreement with other researcher reports [24]. The broadening of the diffraction peaks demonstrated that the powders were a nanostructure form. The nanostructure crystallites were commonly observed as residing of the two structural distinct [25]. Especially, a remarkable fraction of atoms was characterized at the strained exterior for a single–crystal grain core and a surface shell layer. Moreover, the scattering centres produced some fringes that conclusively become "diffraction". At low interference, these fringes started off very broad range and at infinite interference it becomes indefinitely sharp. So, the determination of crystalline size was normally limited to the use of peak broadening. The strain was the other source of specimen broadening. If the crystallite

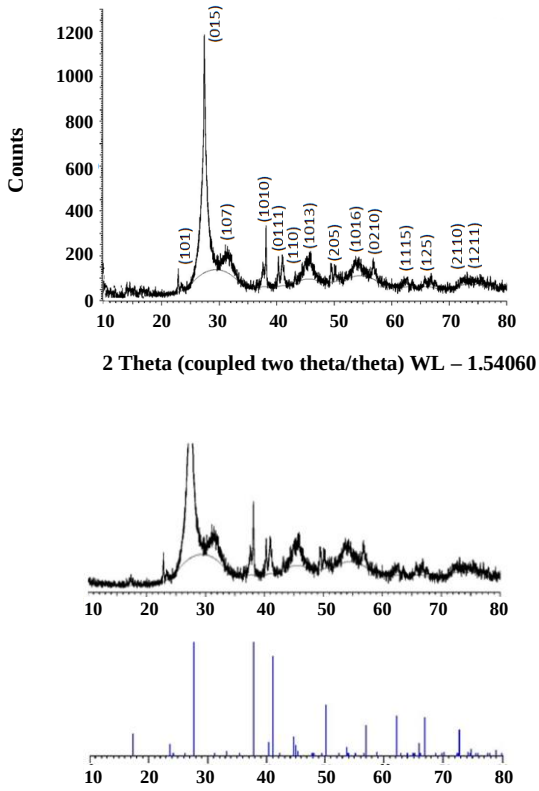

Fig. 1: XRD spectra of prepared Bi_2Te_3 powders.

is strained, then, the d spacing's will be changed; a compressive stress would make the d spacing's smaller, say reducing a given spacing d to d−δd.

The structural defects such as vacancies, interstitials, dislocations and layer faults induced inhomogeneous strain within crystalline materials. The degree of strain was obviously greater at distances closing to the actual defect. X–ray diffractogram provided a wealth of structural information about the nanomaterials. The micro and nanostructure materials were given by fundamental features such as the crystallite size, size distribution, the defect structure, texture, micro and macro strain, etc. The crystalline size and lattice train were estimated with well-known Scherrer equation [26] using the (015) reflection is ~9.25 nm and 0.0164, respectively, that confirmed reasonably well to the literature value [27].

The smallest crystallite material performed the lowest thermal conductivity and high resistivity. It had a crucial effect on the TE figure of merit, *ZT*. Recently, TE applications have attracted increasing interest due to its capability of converting

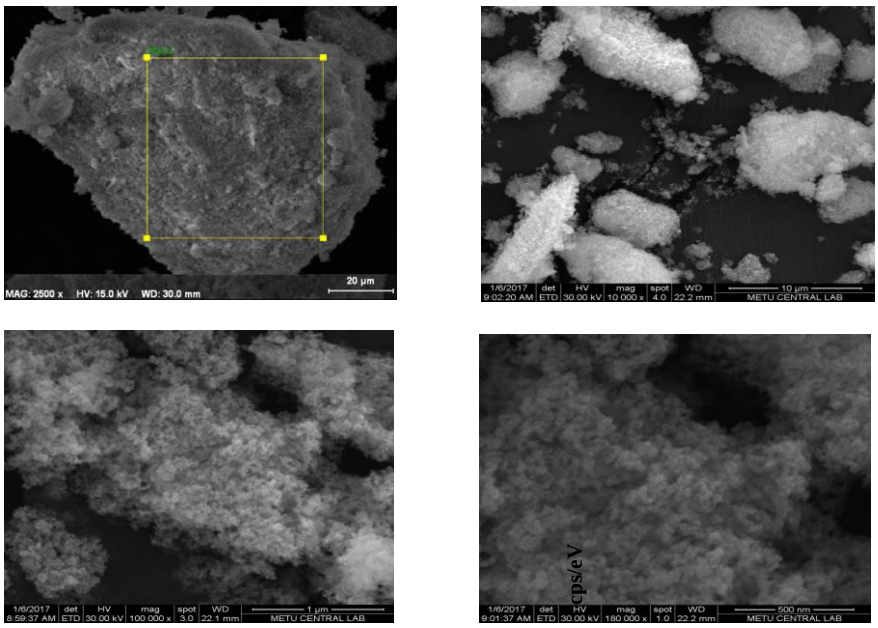

(a) SEM images

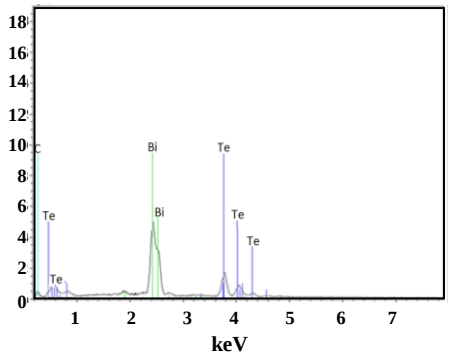

(b) EDX spectrum

Fig. 2: SEM images and EDX spectrum of the prepared Bi_2Te_3 nanostructure.

waste heat into electricity. In this overview, specifically the low dimensional materials are suitable for TE applications.

On the other hand, a SEM image was applied to determine the morphological and microstructural information about the prepared sample. Fig. 2 shows SEM images of the prepared Bi_2Te_3 nanostructure. Its homogeneity was arranged sequentially. This shows that the nanostructure is well agglomerated. It could be seen that the grains of Bi_2Te_3 exhibited initial powder morphologies, quasi spherical granule shapes in agglomerated clusters. The grain size were still in nanometer range according to the other researcher report [28].

Experiments suggested that the behaviour was related to grain boundaries. It indicated a stacking of nanosized particles and crystalline form with broad smooth surfaces to the crystallographic axis. Notably, an influence on the TE properties of this nanostructuration involved a bounding surface boundaries that were impeachable for broad phonon scattering circumstance. Also, the experimental results suggested that the microstructure of the scattering gave a critical consequence on the TE properties. Furthermore, the Bi_2Te_3 nanostructure would be able to achieve a high electrical conductivity and a power factor.

In another measurement, an EDX was utilized to identify the atomic elemental composition of Bi_2Te_3 nanostructure. The EDX analysis was also crucial for improving accuracy of the quantitative compounds. Fig. 2b shows the EDX spectrum that materials of Bi and Te were arranged with their atomic stoichiometric ratio. The atomic composition of Bi and Te elements was approximately 2:3 (30.15):(48.19) within an instrumental accuracy. It was confirmed that the nanostructure was composed of only Bi and Te. The significant increase of an order of magnitude in figure of merit at low temperature was compared to the stoichiometric sample.

The Bi_2Te_3 is one of the promising candidates for TE applications due to its stoichiometric behaviour. However, its energy conversion performance is enhanced by its high thermal conductivity. The above result also shows the other peak which was carbon that indicated the small amount of contamination of the sample. For this reason, the H_2 gas was passed throughout the sample at ~250ºC that the effects of post–depositional contamination. The oxygen containing functional groups were almost reduced in the procedure of reduction with $NaBH_4$. Thus, the metal ions were transformed into the Bi_2Te_3 nanostructure form. Eventually, the nanostructure material was enhanced for the TE power because of the quantum confinement. The size effect led to a carrier confinement. The selective scattering and the interface scattering was reduced. Additionally, the thermal conductivity was improved more than the electrical conductivity. Hence, the figure of merit can be increased in the Bi_2Te_3 nanostructure. On the other hand, contamination might be artificially produced, it occurs in the post–depositional environment. From these curves, it was also confirmed that the Bi_2Te_3 nanostructure was identified Bi and Te which was in good agreement with other researcher report [29]. A key feature of the microstructure was the homogeneous distribution of Bi the Te.

Fig. 3 shows the TEM micrographs of the Bi_2Te_3 nanostructure. The nanostructure exhibited an aggregate phenomenon, and the primary crystalline size was a low dimension. The mean crystalline size distribution was quite narrow. The crystals were connected *via* van-der-Waals forces, but not sintered together. Crystals in this dimension regime had about 50% of their atoms at the surface. From the XRD measurement, the investigation of the full width half maxima (FWHM) intensified in a crystallite size of ~9.25 nm. This was the best reconciliation with the crystalline size measured from the TEM image. In nanostructure materials, the effective scattering of acoustic phonons of the medium frequency with mean free path must be less than 100 nm. The contribution of phonons with mean free path between 5 and 100 nm has occurred about 55% of general scattering. Hence, the features could cause significant reduction in the thermal conductivity of TE behaviour.

About the crystallization, the roughness value of the manufactured pellets was observed by AFM studies that shown in Fig. 4. The AFM is developed to obtain a 3D image of a material surface on an ultramicroscopic scale. The AFM spectra showed that the sample had a nanostructure and uniform grains. There was not anomalous broad crystallization and the appearance of crystalline size was narrow. The surface texture was a crucial issue to interpret the nature of material surfaces. It was the random or repetitive deviation from the ordinary surface that forms the 3D topography of a surface. It plays a crucial role for the functional accomplishment of many scientific applications. It has a portrait that has shorter roughness properties are removed or filtered out and it also does not include any portrait transition due to transition in work piece geometry. So, it is significant to understand that it is always related to roughness when it comes to waviness. The waviness and average spacing between waviness peaks was determined from this profile. The waviness height which was the height from the top of the peak to the bottom of the trough was also defined from this profile. The average roughness height was usually at least three times. The surface roughness value is depends on the scale of measurement. Moreover, the concept of roughness value has a statistical implication that takes into the sample dimension and sampling interval.

Material with a narrow crystalline size was appreciated to maximize the potential for grain boundary. The nanostructure materials indicated a high strength and low ductility properties of the sample. It was recommended that a more superconductive exterior might help to advance the precursor decompositions. This facilitated the formation of exterior complexes that were well confirmed with other researcher report [30]. The average roughness value was about 58 nm which was

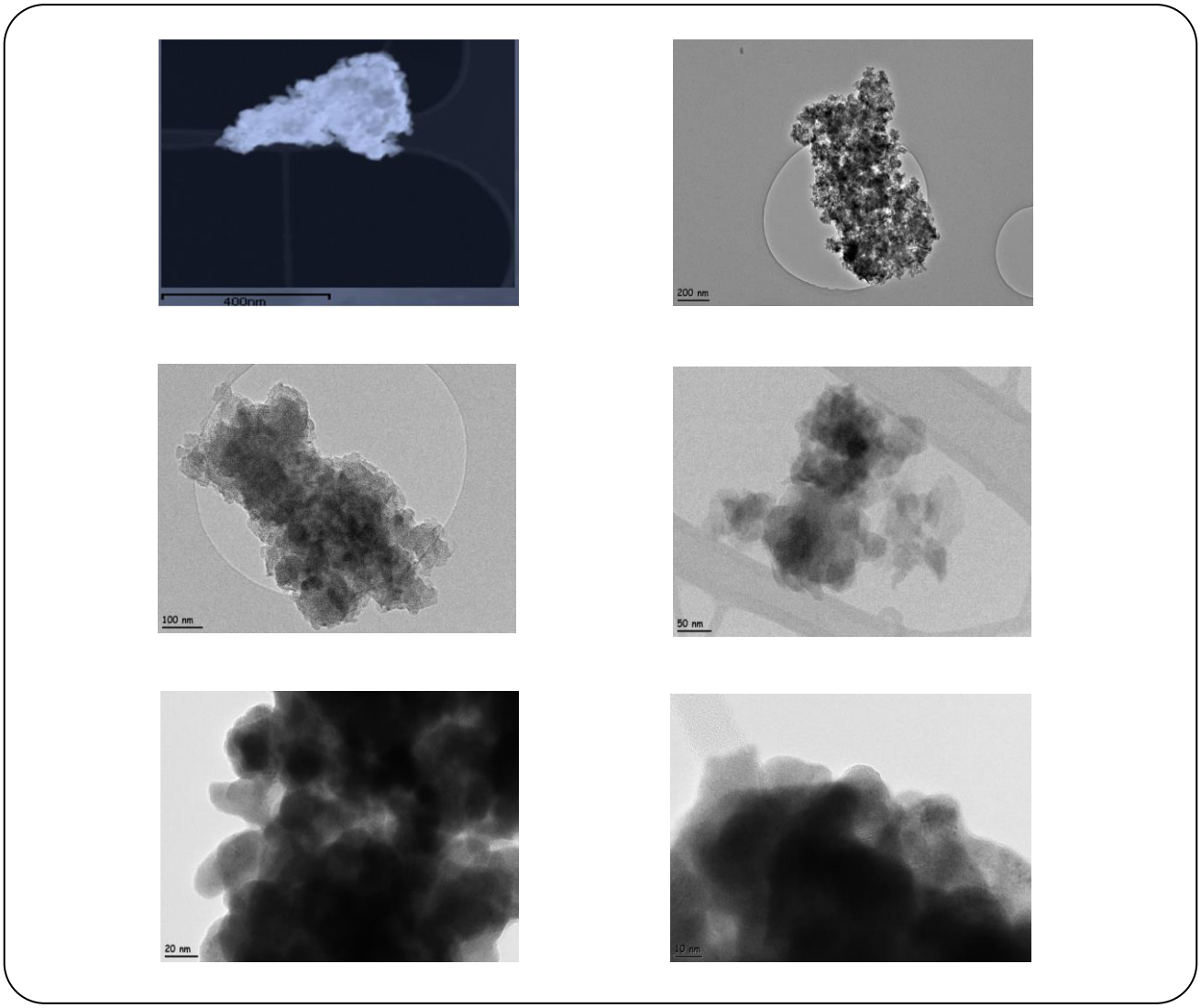

Fig. 3: TEM micrographs of the Bi_2Te_3 nanostructure.

the mean value of the surface fluctuations relative to the centre plane of the sample. The low dimensional (~68 nm) surface roughness value was a strong repercussion for the TE behaviour of nanostructure materials.

The proper distribution of atom on the surface in nanostructure materials as well as their shape has a significant phenomenon on its characteristics. The results might sign that the grains were well arranged and therefore the prepared sample had the lowest scattering coefficient which leads to better conductivity. The boundary grains that could be clearly seen in the image and the results recommended that the electrical conductivity might be improved. The UltraViolet (UV) absorbance - visible absorption spectrum was recorded between 200 and 800 nm for the prepared sample. The absorbance spectrum is shown in Fig. 5 for the Bi_2Te_3 nanostructure.

The exceptional absorption of the Bi_2Te_3 nanostructure was found between 200 and 242 nm that might be due to the quantum incarceration consequence in nanostructure materials. The light moves to the blue end of the spectrum, as its wavelengths get shorter that represent the 'blue shift' formation. The blue shift might be caused by nano dimensional effect [31]. These values were calculated by using the simply Planck equation into the photon energy ranges between 5.1658 and 6.1990 eV, respectively. The shorter wavelengths of light were more energetic than longer wavelengths. The ultra violet

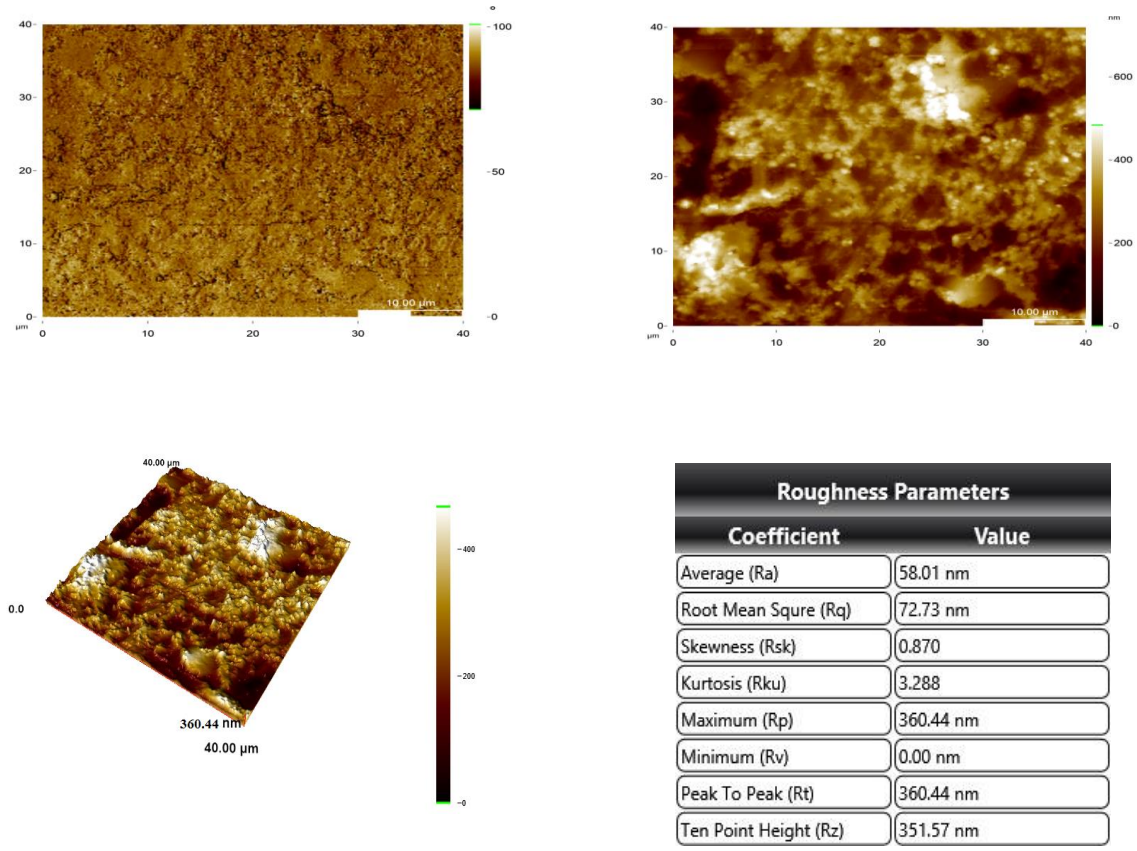

Roughness Parameters	
Coefficient	Value
Average (Ra)	58.01 nm
Root Mean Squre (Rq)	72.73 nm
Skewness (Rsk)	0.870
Kurtosis (Rku)	3.288
Maximum (Rp)	360.44 nm
Minimum (Rv)	0.00 nm
Peak To Peak (Rt)	360.44 nm
Ten Point Height (Rz)	351.57 nm

Fig. 4: AFM image of Bi_2Te_3 nanostructure pellet.

radiation had a low power of penetration. Especially in the range between 30 and 315 nm for nanostructure materials the direct and indirect energy gaps were observed. The similar absorption spectra of doped Bi_2Te_3 nanostructure were observed by the other researcher report [32]. The electron affinity activity was performing between 3.7 and 4.2 eV of the Bi_2Te_3 nanostructure.

The Fourier Transform InfraRed (FT-IR) spectrometry analysis process uses infra-red light to scan the test sample and investigate the chemical behaviour of the materials. Fig. 6 shows the FT-IR transmittance spectra of the Bi_2Te_3 nanostructure. The chemical bonds had characteristic frequencies at which they vibrate. They could be set on vibrations by illuminating the sample with infra-red light at the right frequency.

It can be seen from the Fig. 6 that corresponding to peaks at 2976.97 cm^{-1}, 2662.93 cm^{-1}, 1392.75 cm^{-1} and 634.10 cm^{-1} were assigned to C–H, O–H and C–S stretching, respectively on the prepared sample. The peaks at 2326.01 cm^{-1}, 2115.34 cm^{-1} and 1992.54 cm^{-1} were assigned to triple bond regime of C≡C and C≡N. Other identified major peaks being at 1265.85 cm^{-1}, 949.47 cm^{-1} and 493.43 cm^{-1} were assigned to the finger print. The FTIR spectrums comparing with the reference Bi_2Te_3 nanostructure showed that the C–H, O–H and C–S stretching were well matched [33].The C–H stretching vibrations of the small close cage molecules occurred at a very high frequencies between 3160 and 3100 cm^{-1}, and their low intensities suggested that these bonds were almost homo polar. The C-H bond strengths were following the sequence of lower to higher order. The expected trend of larger vibration shows the correlation between the B-H stretching frequencies and the coupling constants. The most significant feature for the observed

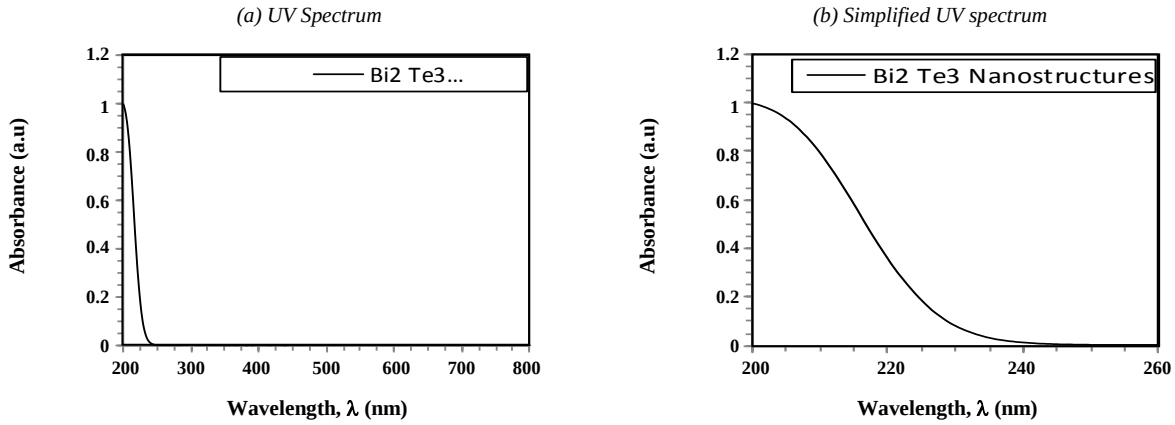

Fig. 5: UV spectrum of the prepared Bi_2Te_3 nanostructure.

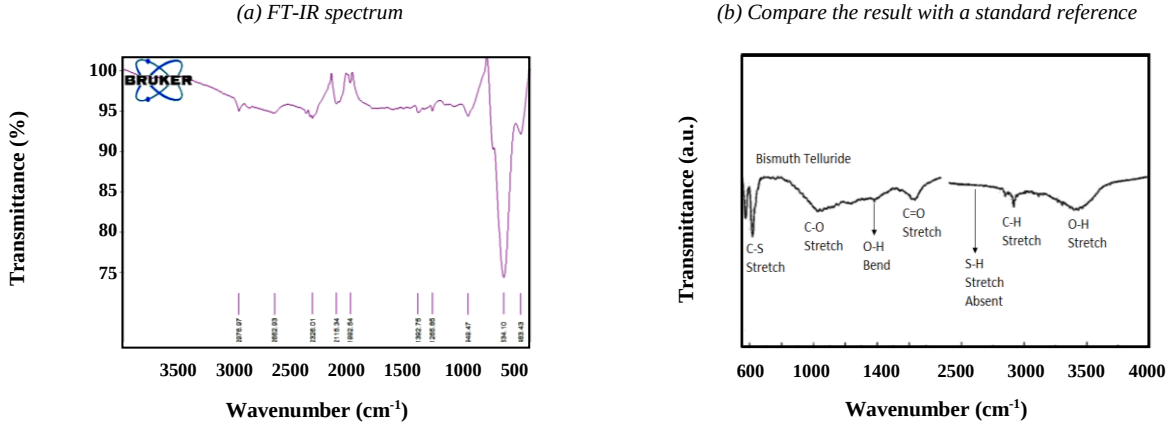

Fig. 6: FT-IR spectra of the Bi_2Te_3 nanostructure.

cage was the having high energy feature. This reflected a strong bonding within the framework of rigid polyhedral molecules having all triangular faces and was consistent with the relatively high barriers. The C-S stretching vibration was assigned to a weak band between 700 and 600 cm^{-1} in the region. The band shows the splitting due to vibration coupling. The O-H stretching vibration of alcohols was easily seen as a strong broad absorption in the spectrum between 3600 and 3400 cm^{-1} region. The chemical shift of hydrogen atoms bonded to the carbon atom bearing the oxygen atom of alcohol occurred in this region. A carbon atom of alcohol had a chemical shift that reflected the shielding of the electronegative oxygen atom.

CONCLUSIONS

In summary, a simple two-step co-precipitation chemical solution route was developed and appropriately established to synthesize the Bi_2Te_3. The precursor was reduced by $NaBH_4$ to produce a fine-particle. The experimental results revealed that the sample exhibited the nanostructure form of crystalline size of about 10 nm. This process was easy, adequate, less precarious and acceptable correlates to the other route. The characterizing aspects of the performed procedure were satisfactory for developing the Bi_2Te_3 nanostructure. Finally, many device quality Bi_2Te_3 nanostructure materials would be developed by using this procedure. It could be easily applicable on TE applications. This research work might open up a way for exploring high-performance of TE materials.

Acknowledgment

This research work is supported by the Scientific and Technological Research Council of Turkey under grant of

TÜBİTAK 2221 Fellowship Program (Ref No: 21514107–115.02–E.69236) and Scientific Research Project Office of Manisa Celal Bayar University (No: 2016-147).

Received : Aug. 14, 2018 ; Accepted : Mar. 11, 2019

REFERENCES

[1] Nassary M.M., Shaban H.T., El–Sadek M.S., Semiconductor Parameters of Bi_2Te_3 Single Crystal, *Materials Chemistry and Physics*, **113**(1): 385-388 (2009).

[2] Snyder G.J., Toberer E.S., Complex Thermoelectric Materials, *Materials for Sustainable Energy*, **7**: 101-110 (2010).

[3] Elsheikh M.H., Shnawah D.A., Sabri M.F.M., Said S.B.M., Hassan M.H., Bashir M.B.A., Mohamad M., A Review on Thermoelectric Renewable Energy: Principle Parameters that Affect Their Performance, *Renewable and Sustainable Energy Reviews*, **30**: 337-355 (2014).

[4] Tenorio H.C.R.L., Vieira D.A., De Souza C.P., Measurement of Parameters and Degradation of Thermoelectric Modules, *IEEE Instrumentation & Measurement Magazine*, **20**(2): 13-19 (2017).

[5] Man E.A., Schaltz E., Rosendahl L., Rezaniakolaei A., Platzek D., A High Temperature Experimental Characterization Procedure for Oxide–Based Thermoelectric Generator Modules Under Transient Conditions, *Energies*, **8**(11): 12839-12847 (2015).

[6] M. Hong, Z.G. Chen, L. Yang, and J. Zou, Enhancing Thermoelectric Performance of Bi_2Te_3 Based Nanostructures Through Rational Structure Design, *Nanoscale*, **16**: 8681-8686 (2016)

[7] Mamur H., Bhuiyan M.R.A., Korkmaz F., Nil M, A Review on Bismuth Telluride (Bi_2Te_3) Nanostructure for Thermoelectric Applications, *Renewable and Sustainable Energy Reviews*, **82**(3): 3047-3052 (2018).

[8] Bhuiyan M.R.A., Mamur H., Review of the Bismuth Telluride (Bi_2Te_3) Nanoparticle: Growth and Characterization, *International Journal of Energy Applications and Technologies*, **3**(2): 27-31 (2016).

[9] Al-Dahash G., Khilkala W.M., Abd Alwahid S.N., Preparation and Characterization of ZnO Nanoparticles by Laser Ablation in NaOH Aqueous Solution, *Iranian Journal of Chemistry and Chemistry Engineering (IJCCE)*, **37**(1): 11-16 (2018).

[10] Mansouri G., Mansouri M., Synthesis and Characterization of Co-Mn Nanocatalyst Prepared by Thermal Decomposition for Fischer-Tropsch Reaction, *Iranian Journal of Chemistry and Chemistry Engineering (IJCCE)*, **37**(3): 1-9 (2018).

[11] Chen S., Cai K., Shen S., Synthesis *via* a Microwave–assisted Wet Chemical Method and Characterization of Bi_2Te_3 with Various Morphologies, *Journal of Electronic Materials*, **45**(3): 1425-1432 (2016).

[12] Takashiri M., Kai S., Wada K., Takasugi S., Tomita K., Role of Stirring Assist during solvothermal Synthesis for Preparing Single–Crystal Bismuth Telluride Hexagonal Nanoplates, *Materials Chemistry and Physics*, **173**: 213-218 (2016).

[13] Liang Y., Wang W., Zeng B., Zhang G., He Q., Fu J., Influence of NaOH on the Formation and Morphology of Bi_2Te_3 Nanostructures in a Solvothermal Process: from Hexagonal Nanoplates to Nanorings, *Materials Chemistry and Physics*, **129**(1–2): 90-98 (2011).

[14] Díaz O.C., de Melo Pereira O., Echavarría A.E., Substrate Influence on Preferential Orientation of Bi_2Te_3 Layers Grown by Physical Vapor Transport Using Elemental Bi and Te Sources, *Materials Chemistry and Physics*, **198**: 341-345 (2017).

[15] Rashad M.M., El-Dissouky A., Soliman H.M., Elseman A.M., Refaat H.M., Ebrahim A., Structure Evaluation of Bismuth Telluride (Bi_2Te_3) Nanoparticles with Enhanced Seebeck Coefficient and Low Thermal Conductivity, *Materials Research Innovations*, **22**(6): 315-323 (2018).

[16] Zhou L., Zhang X., Zhao X., Zhu T., Qin Y., Influence of NaOH on the Synthesis of Bi_2Te_3 *via* a Low-Temperature Aqueous Chemical Method, *Journal of Materials Science*, **44**(13): 3528-3532 (2009).

[17] Yokoyama S., Sato K., Muramatsu M., Yamasuge T., Itoh, T., Motomiya, K., Takahashi, H., Tohji, K., Green Synthesis and Formation Mechanism of Nanostructured Bi_2Te_3 Using Ascorbic Acid in Aqueous Solution, *Advanced Powder Technology*, **26**(3): 789-796 (2015).

[18] Liu Y., Wang Q., Pan J., Sun Y., Zhang L., Song S., Hierarchical Bi_2Te_3 Nanostrings: Green Synthesis and Their Thermoelectric Properties, *Chemistry – A European Journal*, **24**(39): 9765–9768 (2018).

[19] Mamur H., Dilmac O.F., Korucu H., Bhuiyan M.R.A., Cost Effective Chemical Solution Synthesis of Bi_2Te_3 Nanostructure for Thermoelectric Applications, Micro & Nano Letters, **13**(8): 1117-1120 (2018).

[20] Mamur H., Bhuiyan M.R.A., Development of Bismuth Telluride Nanostructure Pellet for Thermoelectric Applications, *Hittite Journal of Science & Engineering*, **5**(4): 293-299 (2018).

[21] Jiang R., Huang T., Liu J., Zhuang J., Yu A., A Novel Method to Prepare Nanostructured Manganese Dioxide and its Electrochemical Properties as a Super Capacitor Electrode, *Electrochimica Acta*, **54**(11): 3047-3052 (2009).

[22] Baruah S., Dutta J., pH–Dependent Growth of Zinc Oxide Nanorods, *Journal of Crystal Growth*, **311**(8): 2549-2554 (2009).

[23] Bhuiyan M.R.A., Hasan S.F., Optical Properties of Polycrystalline $Ag_xGa_{2-x}Se_2$ ($0.4 \leqslant x \leqslant 1.6$) Thin Films, *Solar Energy Materials and Solar Cells*, **91**(2-3): 148-152 (2007).

[24] Sumithra S., Takas N.J., Misra D.K., Nolting W.M., Poudeu P.F.P., Stokes K.L., Enhancement in Thermoelectric Figure of Merit in Nanostructured Bi_2Te_3 with Semimetal Nanoinclusions, *Advanced Energy Materials*, **1**(6): 1141-1147 (2011).

[25] Keshavarz M.K., Vasilevskiy D., Masut R.A., Turenne S., Synthesis and Characterization of Bismuth Telluride–Based Thermoelectric Nanocomposites Containing MoS_2 Nano–Inclusions, *Materials Characterization*, **95**: 44-49 (2014).

[26] Monshi A., Foroughi M.R., Monshi M.R., Modified Scherrer Equation to Estimate More Accurately Nano–Crystallite Size Using XRD, *World Journal of Nano Science and Engineering*, **2**(3): 154-160 (2012).

[27] Kulsi C., Mitra M., Kargupta K., Banerjee D., Thermoelectric Properties of Nanostructured Bismuth Telluride (Bi_2Te_3) with Annealing Time and its Composite with Reduced Graphene Oxide (RGO), *Journal of Materials Science: Materials in Electronics*, 1-11 (2018).

[28] Ivanov O., Maradudina O., Lyubushkin R., Grain Size Effect on Electrical Resistivity of Bulk Nanograined Bi_2Te_3 Material, *Materials Characterization*, **99**: 175-179 (2015).

[29] Benjamin S.L., de Groot C.H., Gurnani C., Hector A.L., Huang R., Koukharenko E., Levason W., Reid G., Controlling the Nanostructure of Bismuth Telluride by Selective Chemical Vapour Deposition from a Single Source Precursor, *Journal of Materials Chemistry A*, **2**(14): 4865-4869 (2014).

[30] Krumrain J., Mussler G., Borisova S., Stoica T., Plucinski L., Schneider C.M., Grützmacher D., MBE Growth Optimization of Topological Insulator Bi_2Te_3 Films, *Journal of Crystal Growth*, **324**(1): 115-118 (2011).

[31] Srivastava P., Singh K., Low Temperature Reduction Route to Synthesis Bismuth Telluride (Bi_2Te_3) Nanoparticles: Structural and Optical Studies, *Journal of Experimental Nanoscience*, **9**(10): 1064-1074 (2014).

[32] Srivastava P., Singh K., Effects of Cs–doping on Morphological, Optical and Electrical Properties of Bi_2Te_3 Nanostructures, *Materials Letters*, **136**: 337-340 **(**2014).

[33] Fu J., Song S., Zhang X., Cao F., Zhou L., Li X., Zhang H., Bi_2Te_3 Nanoplates and Nanoflowers: Synthesized by Hydrothermal Process and Their Enhanced Thermoelectric Properties, *Cryst. Eng. Comm*, **14**(6): 2159-2165 (2012).